Supplemental Figures

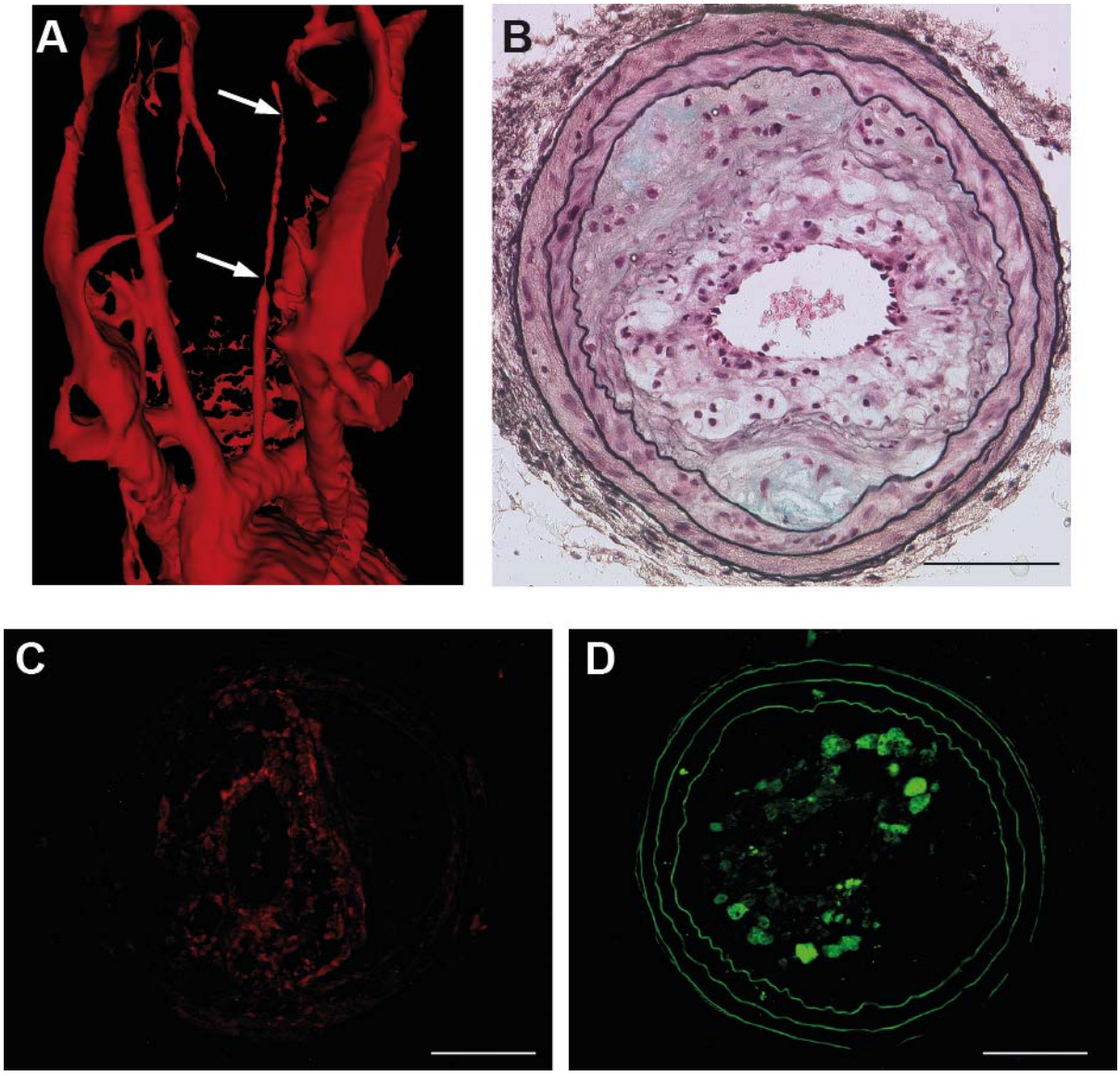

Supplemental Figure 1: Lesion formation in the carotid arteries of *Apoe*$^{-/-}$ mice following partial ligation. (A) Partial carotid ligation in *Apoe*$^{-/-}$ mice results in flow-induced formation of stenotic plaques as detected by micro-CT. A representative 3D reconstruction image is shown. Arrows indicate high-grade stenoses. (B) Histological image of carotid plaques 6 wk after partial ligation. (C) Immunostaining of SMC-specific TAGLN demonstrates lesional SMCs (red). (D) Immunostaining of macrophage-specific MAC2 shows infiltration of the lesion by macrophages (green). Scale bars: 100 µm.

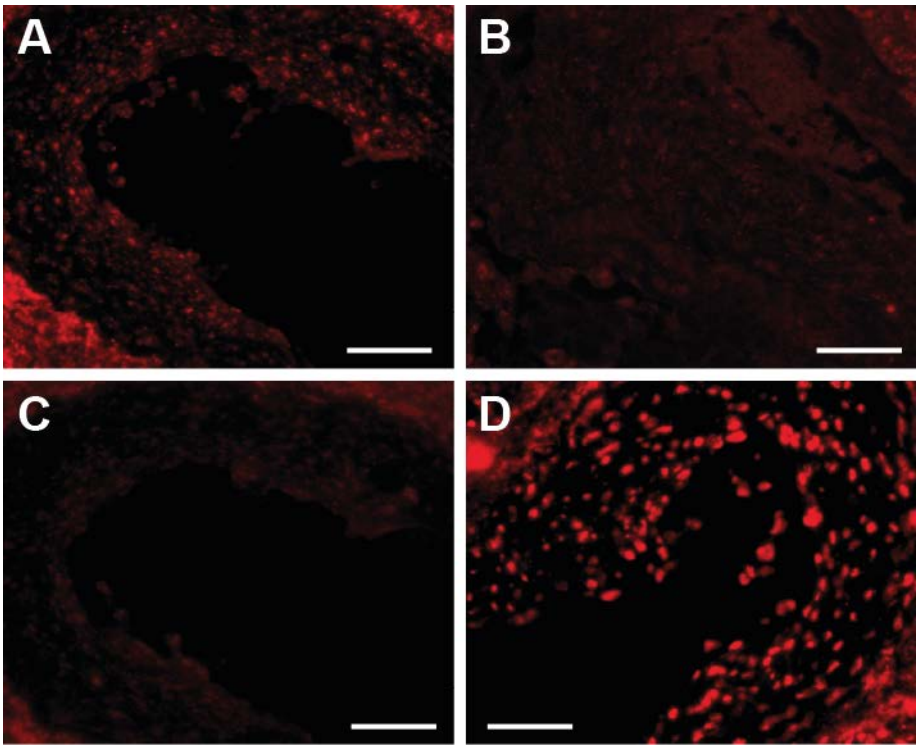

Supplemental Figure 2: Localization of miR-155 in murine atherosclerotic plaques. (A) MiR-155 was detected by in situ hybridization in atherosclerotic plaques induced by partial carotid ligation in *Apoe*$^{-/-}$ mice. (B) MiR-155 was not detectable in carotid plaques of *Mir155*$^{-/-}$*/Apoe*$^{-/-}$ mice. (C) A scrambled probe showed only negliglible background staining in *Apoe*$^{-/-}$ mice. (D) A *U6*-specific probe was used as a positive control for in situ hybridization. Scale bars: 50 µm.

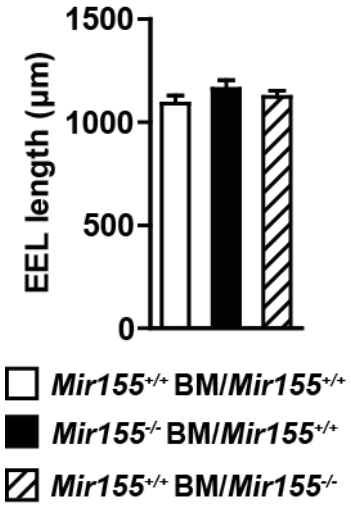

Supplemental Figure 3: Effect of miR-155 on vascular remodeling. The length of the external elastic lamina (EEL) was measured in EVG-stained sections of carotid arteries 6 wk after partial ligation in *Apoe*$^{-/-}$ mice harboring either *Mir155*$^{+/+}$/*Apoe*$^{-/-}$ (*Mir155*$^{+/+}$ BM/*Mir155*$^{+/+}$) or *Mir155*$^{-/-}$/*Apoe*$^{-/-}$ (*Mir155*$^{-/-}$ BM/*Mir155*$^{+/+}$) BM and in *Mir155*$^{-/-}$/*Apoe*$^{-/-}$ mice harboring *Mir155*$^{+/+}$/*Apoe*$^{-/-}$ BM (*Mir155*$^{+/+}$ BM/*Mir155*$^{-/-}$). *n* = 6–8 mice per group. Data represent the mean ± SEM.

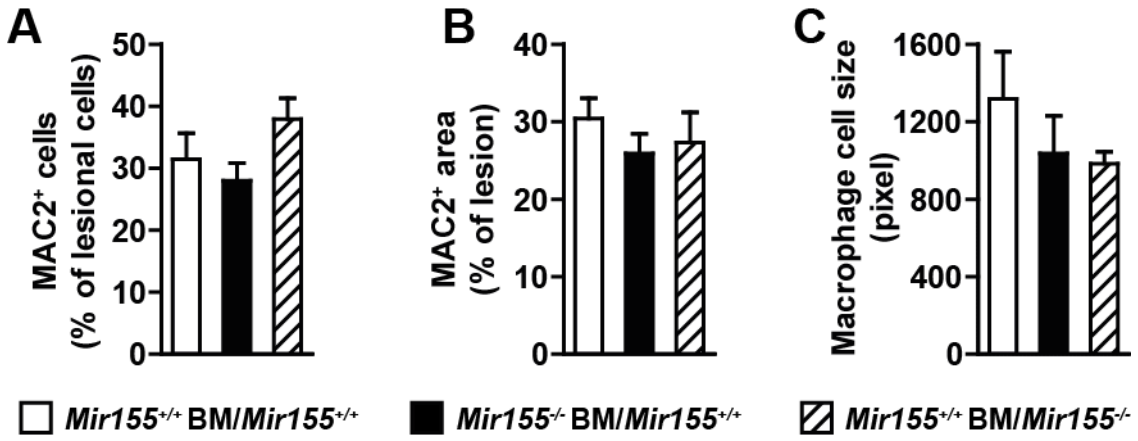

Supplemental Figure 4: Effect of miR-155 deficiency on lesional macrophages. The relative number of MAC2-positive cells (A), relative MAC2-positive area (B), and macrophage cell size (C) were determined by macrophage-specific MAC2 immunostaining in carotid plaques induced by partial ligation in *Apoe*$^{-/-}$ mice harboring either *Mir155*$^{+/+}$*/Apoe*$^{-/-}$ (*Mir155*$^{+/+}$ BM/*Mir155*$^{+/+}$) or *Mir155*$^{-/-}$*/Apoe*$^{-/-}$ (*Mir155*$^{-/-}$ BM/*Mir155*$^{+/+}$) BM and in *Mir155*$^{-/-}$*/Apoe*$^{-/-}$ mice harboring *Mir155*$^{+/+}$*/Apoe*$^{-/-}$ BM (*Mir155*$^{+/+}$ BM/*Mir155*$^{-/-}$). *n* = 6–8 mice per group. Data represent the mean ± SEM.

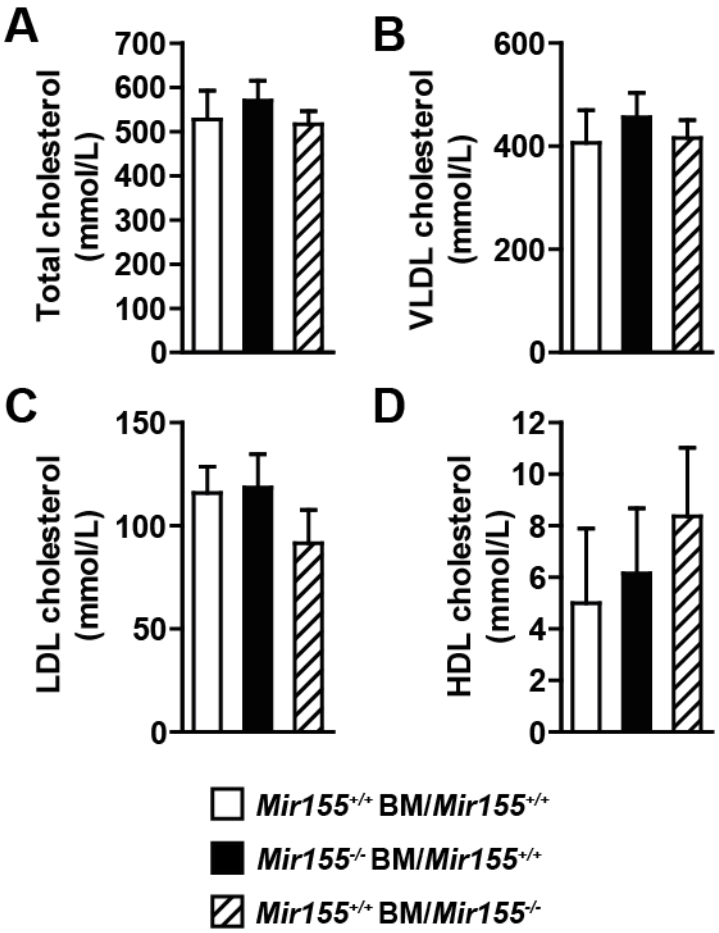

Supplemental Figure 5: Role of miR-155 deficiency on the plasma lipoprotein profile. The plasma levels of total, VLDL, LDL, and HDL cholesterol were determined by HPLC in *Mir155*$^{+/+}$*/Apoe*$^{-/-}$ mice harboring either *Mir155*$^{+/+}$*/Apoe*$^{-/-}$ (*Mir155*$^{+/+}$ BM/*miR-155*$^{+/+}$) or *Mir155*$^{-/-}$*/Apoe*$^{-/-}$ (*Mir155*$^{-/-}$ BM/*Mir155*$^{+/+}$) BM and in *Mir155*$^{-/-}$*/Apoe*$^{-/-}$ mice harboring *Mir155*$^{+/+}$*/Apoe*$^{-/-}$ (*Mir155*$^{+/+}$ BM/*Mir155*$^{-/-}$) BM after 6 wk of feeding a HFD. *n* = 4–8 mice per group. Data represent the mean ± SEM.

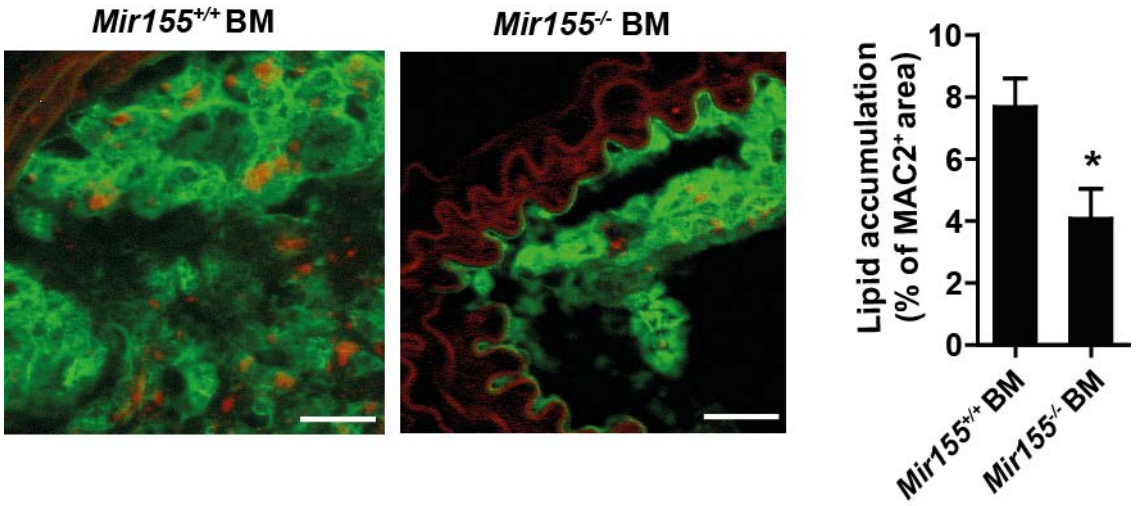

Supplemental Figure 6: Lipid accumulation is reduced in lesional *Mir155*$^{-/-}$ macrophages. Combined immunostaining for MAC2 (green) and with Oil red O (red) was performed in sections of partially ligated carotid arteries from *Mir155*$^{+/+}$*/Apoe*$^{-/-}$ mice harboring either *Mir155*$^{+/+}$*/Apoe*$^{-/-}$ (*Mir155*$^{+/+}$ BM) or *Mir155*$^{-/-}$*/Apoe*$^{-/-}$ (*Mir155*$^{-/-}$ BM) BM. Representative images are shown. The Oil red O-stained area per MAC2^{+} area was quantified. *n* = 3–4 mice per group. **P* < 0.05. Scale bars: 20 µm. Data represent the mean ± SEM.

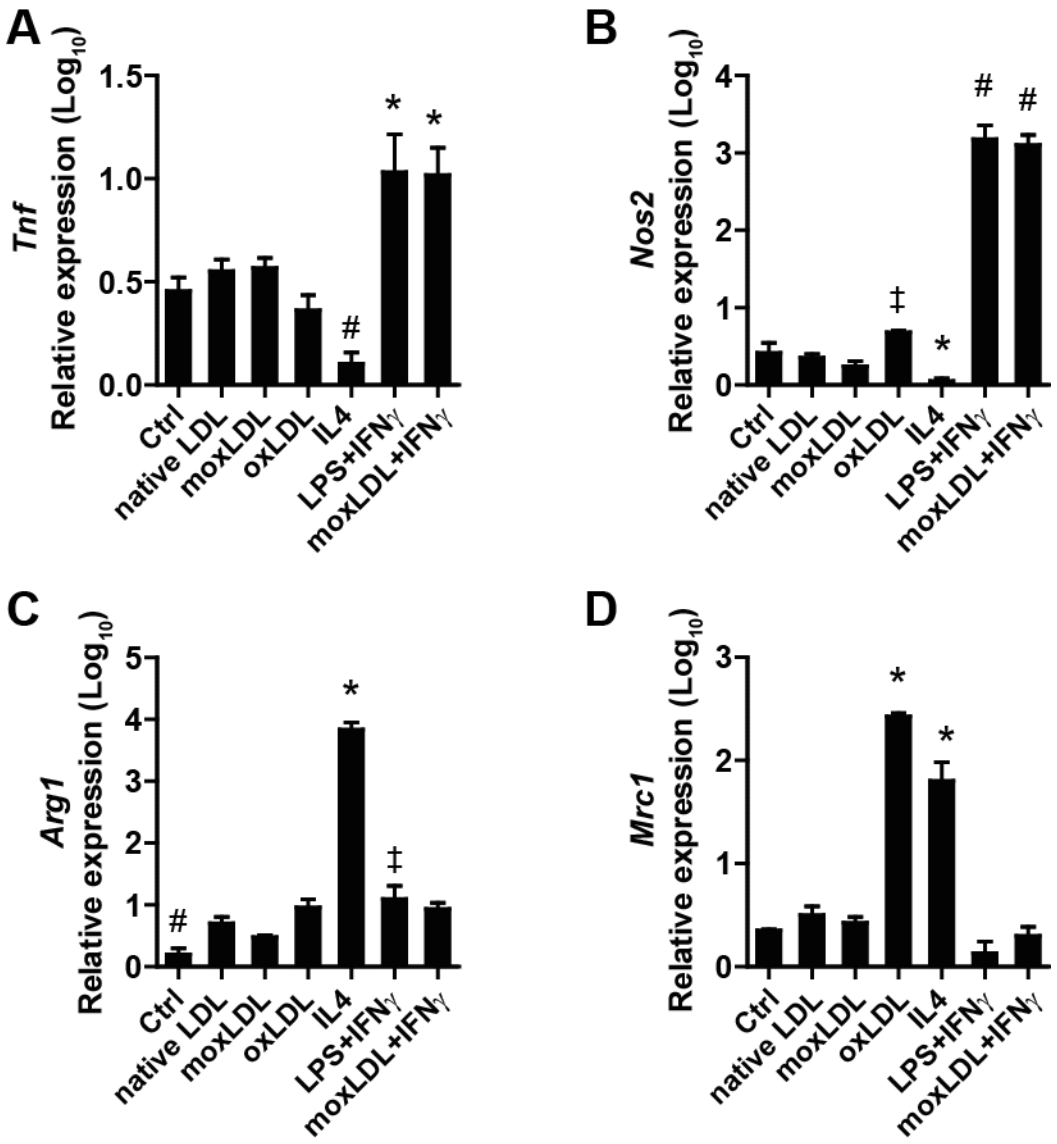

Supplemental Figure 7: Expression of M1- and M2-type macrophage markers following atherogenic stimulation. (A) *Tnf* mRNA expression was quantified in BMDMs after stimulation. **P* < 0.05 versus control (Ctrl), native LDL, moxLDL, oxLDL, and IL4; #*P* < 0.05 versus native LDL, moxLDL, LPS + IFNγ, and moxLDL + IFNγ. (B) The expression of *Nos2* was studied by quantitative RT-PCR in BMDMs after stimulation as indicated. **P* < 0.05 versus oxLDL, LPS + IFNγ, and moxLDL + IFNγ; #*P* < 0.05 versus Ctrl, native LDL, moxLDL, oxLDL, and IL4; ‡*P* < 0.05 versus moxLDL. The expression of the M2-type markers, *Arg1* (C) and *Mrc1* (D), was analyzed in BMDMs. **P* < 0.05 versus all other groups; #*P* < 0.05 versus native LDL, oxLDL, IL4, LPS + IFNγ, and moxLDL + IFNγ; ‡*P* < 0.05 versus moxLDL. Three independent experiments were conducted per group. Data represent the mean ± SEM.

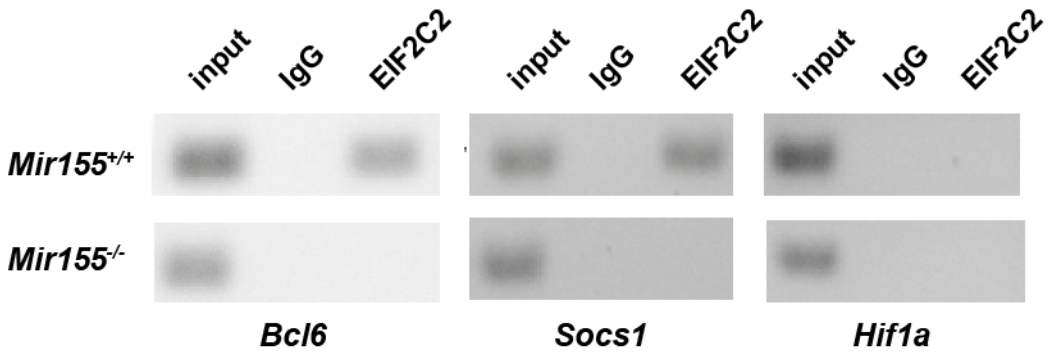

Supplemental Figure 8: Identification of miR-155 targets in stimulated BMDMs. IP of the mRISC protein, EIF2C2, using a specific antibody showed enrichment of *Bcl6* and *Socs1* mRNA in *Mir155*$^{+/+}$ BMDMs compared with *Mir155*$^{-/-}$ BMDMs. The miR-155 target, *Hif1a*, was not detectable by EIF2C2 IP of *Mir155*$^{+/+}$ or *Mir155*$^{-/-}$ BMDMs. In the negative control experiments, non-specific IgG did not precipitate any miR-155 targets. Representative images of agarose gels are shown.

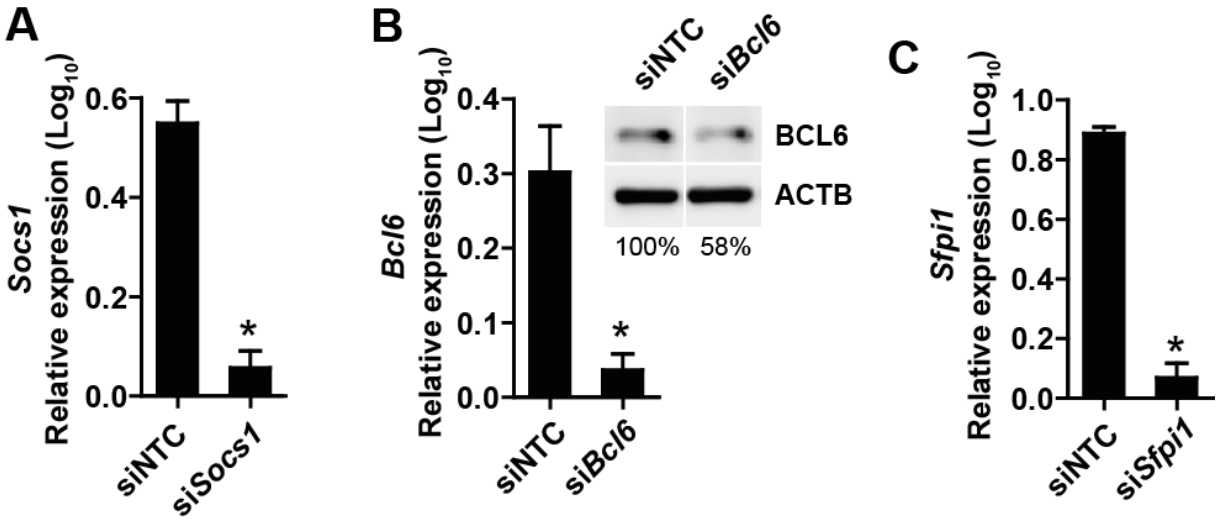

Supplemental Figure 9: Confirmation of siRNA-mediated downregulation of potential miR-155 targets. The expression of *Socs1* (A), *Bcl6* (B), and *Sfpi1* mRNA (C) was quantified by qRT-PCR in BMDMs stimulated with moxLDL and IFNγ and treated with non-targeting siRNA (siNTC) or siRNA against *Socs1* (si*Socs1*, A), *Bcl6* (si*Bcl6*, B), and *Sfpi1* (si*Sfpi1*, C). (B) Western blot analysis was performed to detect BCL6 protein in BMDMs treated with siNTC or si*Bcl6*. The band intensities normalized to that of ACTB are shown. Lanes were run on the same gel but were noncontiguous. Three independent experiments were conducted for each group. **P* < 0.05. Data represent the mean ± SEM.

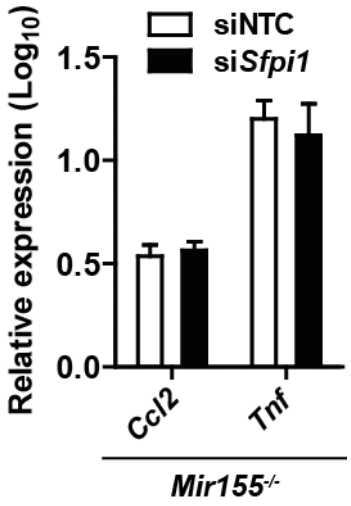

Supplemental Figure 10: Role of *Sfpi1* in the regulation of miR-155-mediated cytokine expression. The expression of *Ccl2* and *Tnf* mRNA in *Mir155*$^{-/-}$ BMDMs was quantified by qRT-PCR following treatment with non-targeting control siRNA (siNTC) or siRNA against *Sfpi1*. At least three independent experiments were conducted per group. Data represent the mean ± SEM.

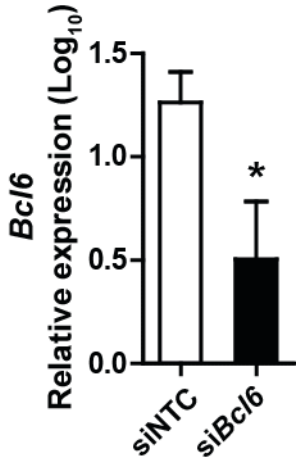

Supplemental Figure 11: Suppression of *Bcl6* mRNA expression in vivo. Partially ligated carotid arteries of *Mir155*$^{+/+}$*/Apoe*$^{-/-}$ mice harboring *Mir155*$^{-/-}$*/Apoe*$^{-/-}$ BM were perivascularly treated once-weekly with siRNA against *Bcl6* (si*Bcl6*) or non-targeting control siRNA (siNTC). The *Bcl6* mRNA expression was determined in the carotid arteries by qRT-PCR. n = 3–4 mice per group. *P < 0.05. Data represent the mean ± SEM.

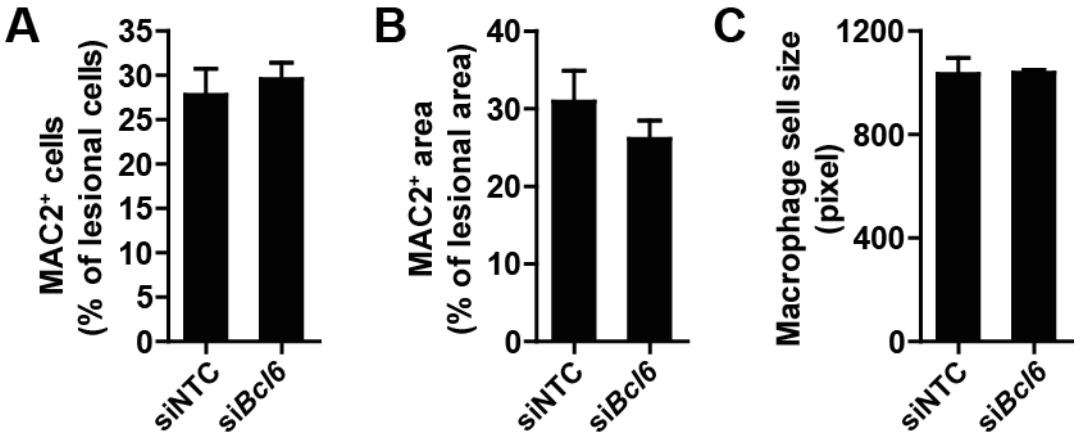

Supplemental Figure 12: Effect of BCL6 on lesional *Mir155*$^{-/-}$ macrophages. Partially ligated carotid arteries from *Mir155*$^{+/+}$*/Apoe*$^{-/-}$ mice harboring *Mir155*$^{-/-}$*/Apoe*$^{-/-}$ BM were perivascularly treated with siRNA against *Bcl6* (si*Bcl6*) or non-targeting control siRNA (siNTC). The relative macrophage cell number (A), the relative lesional macrophage area (B), and the macrophage cell size (C) was determined in carotid artery sections immunostained for MAC2. *n* = 4 mice per group. Data represent the mean ± SEM.

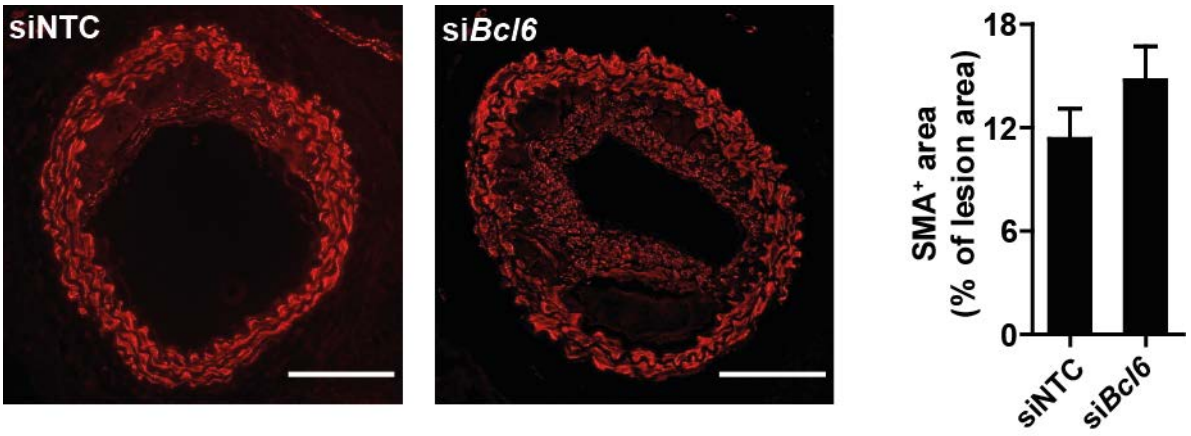

Supplemental Figure 13: Effect of BCL6 on lesional SMCs. Partially ligated carotid arteries from *Mir155*$^{+/+}$*/Apoe*$^{-/-}$ mice harboring *Mir155*$^{-/-}$*/Apoe*$^{-/-}$ BM were perivascularly treated with siRNA against *Bcl6* (si*Bcl6*) or non-targeting control siRNA (siNTC). The relative SMC content in lesions in the carotid arteries was quantified staining sections for SMA (red). *n* = 4 mice per group. Scale bars: 100 µm. Data represent the mean ± SEM.

Supplemental Tables

miRs	-Fold change ($Log_{10}RQ$)	*P* value	Adjusted *P* value
miR-501-3p	3.548	0.0054	0.0183
miR-146b*	2.560	0.0062	0.0207
miR-467d	2.528	0.0142	0.0423
miR-147	2.426	0.0005	0.0042
miR-342-5p	1.530	0.0318	0.0802
miR-582-3p	1.018	0.0379	0.0913
miR-802	0.979	0.0276	0.0724
miR-21	0.798	0.0002	0.0042
miR-34c	0.786	0.0170	0.0485
miR-146b	0.762	0.0007	0.0009
miR-34c*	0.732	0.0086	0.0275
miR-34b-3p	0.713	0.0050	0.0174
miR-155	0.674	0.0010	0.0044
miR-685	0.616	0.0034	0.0127
miR-15b*	0.546	0.0045	0.0160
miR-342-3p	0.537	0.0019	0.0076
miR-142-5p	0.516	0.0012	0.0050
miR-34a	0.489	0.0053	0.0181
miR-142-3p	0.472	0.0024	0.0094
miR-221	0.458	0.0030	0.0111
miR-21*	0.448	0.0005	0.0042
miR-223	0.442	0.0012	0.0051
miR-146a	0.434	0.0017	0.0070
miR-222	0.412	0.0003	0.0042
miR-511	0.341	0.0065	0.0212
miR-184	0.314	0.0271	0.0716
miR-467a	0.251	0.0153	0.0452
miR-31	0.232	0.0244	0.0660
miR-340-5p	0.205	0.0162	0.0472
miR-467b	0.177	0.0099	0.0310
let-7i	0.168	0.0451	0.1065
miR-652	0.144	0.0266	0.0706
miR-484	0.114	0.0367	0.0888

Supplemental Table 1: Up-regulation of miRs in atherosclerotic lesions. MiRs significantly up-regulated in the carotid artery 6 wk after partial ligation in *Apoe*$^{-/-}$ mice fed a HFD for 6 wk compared with the contralateral carotid artery (determined by quantitative RT-PCR array). *P* values were adjusted using the Benjamini-Hochberg procedure. *n* = 6 mice. The –fold change data represent the mean.

miRs	-Fold change ($Log_{10}RQ$)	*P* value	Adjusted *P* value
miR-375	-1.191	0.0076	0.025
miR-201	-0.967	0.0139	0.042
miR-187	-0.814	0.0051	0.018
miR-145	-0.781	0.0036	0.013
miR-378*	-0.755	0.0047	0.016
miR-378	-0.703	0.0033	0.012
miR-143	-0.698	0.0015	0.006
miR-365	-0.618	0.0005	0.004
miR-1	-0.589	0.0022	0.009
miR-107	-0.586	0.0001	0.004
let-7d*	-0.561	0.0043	0.015
miR-193*	-0.485	0.0039	0.014
miR-193	-0.478	0.0121	0.037
miR-193b	-0.460	0.0005	0.004
miR-133b	-0.446	0.0065	0.021
miR-133a	-0.432	0.0090	0.028
miR-29c*	-0.419	0.0001	0.004
miR-224	-0.390	0.0096	0.03
miR-708	-0.389	0.0003	0.004
miR-30c	-0.380	0.0007	0.004
miR-720	-0.373	0.0109	0.034
miR-101a*	-0.369	0.0179	0.0506
miR-30e*	-0.345	0.0000	0.004
let-7g*	-0.344	0.0060	0.02
let-7a*	-0.339	0.0026	0.01
miR-30a*	-0.336	0.0000	0.004
miR-411*	-0.321	0.0231	0.0628
miR-486	-0.318	0.0114	0.035
miR-30b	-0.302	0.0015	0.006
miR-206	-0.302	0.0341	0.0845
miR-33*	-0.301	0.0318	0.0802
miR-485*	-0.300	0.0206	0.0564
let-7a	-0.299	0.0322	0.0806
miR-805	-0.290	0.0029	0.011
miR-99a	-0.289	0.0005	0.001
let-7f	-0.281	0.0121	0.037
miR-28*	-0.267	0.0081	0.026
miR-100	-0.265	0.0002	0.001
miR-467b*	-0.264	0.0485	0.1126
miR-28	-0.263	0.0186	0.0523
miR-182	-0.261	0.0472	0.1101
miR-491	-0.260	0.0247	0.0662
let-7b	-0.256	0.0317	0.0802
miR-328	-0.255	0.0055	0.019
miR-709	-0.252	0.0006	0.004
miR-701	-0.246	0.0308	0.0794
miR-30b*	-0.240	0.0246	0.0662

miR-181a-1*	-0.238	0.0280	0.0731
miR-26b	-0.237	0.0026	0.01
miR-297c	-0.233	0.0453	0.1066
miR-467a*	-0.231	0.0358	0.0874
miR-204	-0.223	0.0087	0.028
miR-301a	-0.203	0.0168	0.048
miR-26b*	-0.203	0.0061	0.02
miR-125b*	-0.200	0.0026	0.01
miR-30e	-0.196	0.0018	0.007
miR-30a	-0.195	0.0156	0.046
let-7c-1*	-0.195	0.0440	0.1050
miR-15a*	-0.193	0.0345	0.0845
miR-23b	-0.191	0.0200	0.0550
miR-673-5p	-0.191	0.0343	0.0845
miR-101b	-0.189	0.0046	0.016
miR-26a	-0.188	0.0166	0.048
miR-24-2*	-0.182	0.0252	0.0673
miR-152	-0.174	0.0496	0.1141
miR-192	-0.173	0.0044	0.0156
miR-301b	-0.173	0.0147	0.044
miR-92a	-0.171	0.0198	0.0548
miR-140	-0.170	0.0416	0.0996
miR-194	-0.167	0.0198	0.0548
miR-376c	-0.158	0.0447	0.1062
miR-379	-0.151	0.0284	0.0734
miR-203	-0.147	0.0030	0.011
miR-29c	-0.145	0.0044	0.016
miR-877*	-0.145	0.0103	0.032
miR-126-5p	-0.139	0.0177	0.0502
miR-7a*	-0.135	0.0165	0.048
miR-27a	-0.132	0.0284	0.0734
miR-361	-0.128	0.0321	0.0806
miR-101a	-0.119	0.0496	0.1141
miR-872*	-0.104	0.0116	0.036
miR-93*	-0.085	0.0192	0.0537
miR-374	-0.050	0.0343	0.0845

Supplemental Table 2: Down-regulation of miRs in atherosclerotic lesions. MiRs significantly down-regulated in the carotid artery 6 wk after partial ligation in *Apoe*$^{-/-}$ mice fed a HFD for 6 wk compared with the contralateral carotid artery (determined using a quantitative RT-PCR array). *P* values were adjusted using the Benjamini-Hochberg procedure. *n* = 6 mice. The –fold change data represent the mean.

miRs	-Fold change ($Log_{10}RQ$)	*P* value	Adjusted *P* value
miR-139-3p	2.754	0.016	0.5728
miR-452	2.127	0.024	0.5951
miR-676*	1.871	0.006	0.3688
miR-10b*	1.347	0.015	0.5728
miR-147	0.952	0.004	0.3454
miR-155	0.933	0.018	0.5728

Supplemental Table 3: Up-regulation of miRs in murine inflammatory macrophages. MiRs significantly up-regulated in BM-derived macrophages (BMDMs) stimulated with LPS and IFNγ compared with unstimulated BMDMs (determined using a quantitative RT-PCR array). *P* values were adjusted using the Benjamini-Hochberg procedure. *n* = 5 independent experiments. The –fold change data represent the mean.

miRs	-Fold change ($Log_{10}RQ$)	*P* value	Adjusted *P* value
miR-466d-3p	-3.648	0.034	0.6557
miR-590-5p	-3.301	0.003	0.3454
miR-302a	-2.230	0.003	0.3454
miR-495	-1.938	0.026	0.5951
miR-376b*	-1.745	0.001	0.3454
miR-383	-1.655	0.042	0.7642
let-7c-1*	-1.230	0.034	0.6557
miR-107	-0.544	0.007	0.3989
miR-15b*	-0.393	0.030	0.6287
miR-106b*	-0.379	0.026	0.5951
miR-411	-0.365	0.004	0.3454
miR-191*	-0.360	0.020	0.5871
miR-805	-0.302	0.023	0.5929
miR-24-1*	-0.297	0.008	0.3989
miR-326	-0.295	0.004	0.3454
miR-501-5p	-0.289	0.005	0.3454
miR-409-3p	-0.270	0.030	0.6287
miR-26b*	-0.264	0.014	0.5728
miR-339-5p	-0.243	0.047	0.7846
miR-27b*	-0.239	0.049	0.7846
miR-15a*	-0.238	0.017	0.5728
miR-24-2*	-0.226	0.022	0.5929
miR-93*	-0.224	0.012	0.5728
miR-340-3p	-0.193	0.043	0.7642
miR-130b*	-0.191	0.020	0.5871
miR-29c*	-0.174	0.046	0.7846

Supplemental Table 4: Down-regulation of miRs in murine inflammatory macrophages. MiRs significantly down-regulated in BM-derived macrophages (BMDMs) stimulated with LPS and IFNγ compared with unstimulated BMDMs as determined by quantitative RT-PCR array. *P* values were adjusted using the Benjamini-Hochberg procedure. *n* = 5 independent experiments. The –fold change data represent the mean.

Supplemental Methods

Human carotid plaque samples

Human atherosclerotic plaque specimens were obtained during carotid endarterectomy and immediately shock-frozen in liquid nitrogen. Frozen carotid artery specimens were macroscopically and separated into plaques and artery wall specimens in liquid nitrogen using a scalpel. Total RNA was then isolated using the mirVana kit (Life Technologies).

Micro-computed tomography (micro-CT)

The carotid arteries of *Apoe*$^{-/-}$ mice were analyzed for luminal stenosis 6 wk after partial ligation of the left carotid artery. A blood pool contrast agent (5 ml/kg) was injected via a tail vein catheter into mice anesthetized with isoflurane. Mice were subsequently scanned with a micro-CT (TomoScope DUO; CT Imaging GmbH, Erlangen, Germany) using a dual energy (40 kV/1mA, 65 kV/0.5 mA) scan protocol, which acquired 2880 projections of 1032 × 1012 pixels over 6 min. Reconstructions with an isotropic voxel size of 35 µm were computed using a modified Feldkamp algorithm. Blood vessels were segmented using dual energy functionality and rendered for visualization. The lumen diameters of left and right common carotid arteries were measured to assess the impact of the partial ligation on the vessel structure.

Quantitative real time RT-PCR

Total RNA was reverse transcribed using a Taqman microRNA RT kit or high capacity cDNA reverse transcription kit. MiRNA qRT-PCR was performed using Taqman microRNA assays and Taqman universal PCR master mix (Life Technologies). QRT-PCR for mRNAs was performed using gene specific primers and SYBR Green master mix (Fermentas). All real-time PCR experiments were run on a 7900HT RT-PCR system. The data were normalized to a single or to multiple reference genes (*snoRNA-135*, *snoRNA-429*, and *U6* for miR; *Gapdh* and *Actb* for mRNA), scaled to the sample with the lowest expression (qbase software; Biogazelle), and logarithmically transformed (Log_{10}).

Preparation of moxLDL

Mildly-oxidized LDL (moxLDL) was prepared as previously described (1). Briefly, human native LDL (1 mg/mL; Calbiochem) was mildly-oxidized at 37°C in the presence of 5 µM $CuSO_4$ for 4 h. The oxidation was stopped at the beginning of the propagation phase by the addition of 10 µM EDTA (final concentration). The LDL was washed with PBS over a PD-10 desalting column (GE Healthcare). After measuring the protein concentration using a DC protein assay kit (Bio-Rad), the LDL was filtered through a 0.45 µm filter and stored at 4°C for a maximum of 14 d. To generate highly oxidized LDL (oxLDL), moxLDL was stored for 4 mo at 4°C. Quantification of the oxidative modifications was performed by measuring conjugated dienes at an optical density of 234 nm (Nanodrop), which showed a 20-fold higher level of oxidation in oxLDL compared with moxLDL.

Cell culture

BM cells were harvested from the femurs of *Mir155*$^{+/+}$*/Apoe*$^{-/-}$ and *Mir155*$^{-/-}$*/Apoe*$^{-/-}$ mice, re-suspended in DMEM-F12 medium supplemented with 10% fetal calf serum and 10% L929-conditioned medium, and cultured for 7 d to allow differentiation into primary macrophages. F4/80 (APC-labeled anti-mouse rat IgG2a; eBiosciences) and CD11b (PerCP-Cy™5.5-labeled anti-mouse rat IgG2b; BD Pharmingen) expression was determined by flow cytometry (FACSCanto II; BD Biosciences) to confirm the macrophage phenotype. Bone marrow-derived macrophages (BMDMs) were stimulated with moxLDL (50 µg/ml, 14 h) and IFNγ (10 ng/ml, 6 h), LPS (100 ng/ml, 14 h) and IFNγ (10 ng/ml, 6 h), IL4 (5 ng/ml, 6 h), moxLDL (50 µg/ml, 14 h), oxLDL (50 µg/ml, 14 h), or native LDL (50 µg/ml, 14 h). MoxLDL and IFNγ-stimulated BMDMs from *Mir155*$^{-/-}$*/Apoe*$^{-/-}$ mice were treated with non-targeting siRNA or siRNA against *Socs1*, *Sfpi1*, and *Bcl6* (500 nM, Accell siRNA in Accell cell culture medium; Dharmacon) on Day 4 and then stimulated with moxLDL and IFNγ on Day 7. Total RNA was isolated using the mirVana microRNA Isolation Kit (Life Technologies). In some experiments a blocking TNFα antibody (5 µg/ml, clone MP6-XT22; R&D Systems) or an isotype control antibody (5 µg/ml; R&D Systems) was added to the medium during stimulation of BMDMs.

Migration assay

Migration of BMDMs was assessed in vitro using a two-chamber migration assay. Unstimulated BMDMs (1×10^5 cells) were plated onto a Matrigel-coated Transwell filter (8 µm pore size; Corning, Inc.) and were allowed to migrate across the porous filter for 24 h at 37°C towards CCL2 (10 ng/ml, Peprotech), which was placed in the lower chamber. After removal of the non-migrating BMDMs from the upper surface, the filter was fixed and stained with DAPI. Migrated BMDMs on the bottom of the filter were counted using a fluorescence microscope. The number of cells that migrated completely across the filter was determined in six random fields (magnification ×100) for each experiment.

Apoptosis assay

Macrophage apoptosis was quantified using a terminal deoxynucleotidyl transferase-mediated biotinylated UTP nick end labeling (TUNEL) assay (Roche Diagnostics GmbH, Roche Applied Science) following the manufacturer's instructions. Briefly, BMDMs were harvested and diluted to 2×10^6 cells/100 µl in PBS for each sample. Following fixation with 2% paraformaldehyde, BMDMs were permeabilized with 0.1% Triton X-100. The labeling reaction was performed by incubating the BMDMs with the labeling solution containing terminal deoxynucleotidyl transferase for 1 h at 37°C. The number of labeled BMDMs was quantified by flow cytometry (FACSCanto, BD Biosciences). Data were analyzed using FlowJo 7.0 software (Tree Star Inc).

Prediction of miR-155s target genes

Potential miR-155 target genes were identified using the following miR target prediction algorithms: TargetScan (2) (***www.targetscan.org***), miRanda (***www.microrna.org***) (3), and MicroCosm Targets (4) (***www.ebi.ac.uk/enright-srv/microcosm/htdocs/targets/v5/***).

Western blot analysis

BMDMs were lysed in 50 mM Tris-Cl (pH 8.0), 150 mM NaCl, 1% Triton X-100, and 2 mM EDTA, supplemented with protease inhibitors (Complete protease inhibitor cocktail, Roche). Total cell lysates were boiled for 10 min in 1× Laemmli loading buffer supplemented with β-mercaptoethanol, resolved on 10% SDS-PAGE gels, and transferred to PVDF membranes. Proteins were detected with antibodies to BCL6 (rabbit polyclonal; Abcam) and β-actin (ACTB, clone AC-15; Sigma-Aldrich) followed by detection with the appropriate HRP-conjugated secondary antibodies (Santa Cruz). Protein bands were visualized using an enhanced chemiluminescence detection system (ECL Advance; GE Healthcare) on a LAS 3000 Imager (Fujifilm) and quantified using Multigauge software.

Enzyme linked immunosorbent assay (ELISA)

The concentration of CCL2 and TNFα was determined in BMDM cell lysates or cell culture medium using a mouse CCL2 Elisa kit or a TNFα Elisa kit (both from Ray Biotech, Inc.,), respectively. The absorbance was measured with a microplate reader (SPECTRAFluor Plus, Tecan).

Lipoprotein profiling

Automated plasma lipoprotein analysis was performed by running 20 µL plasma samples at a flow rate of 0.2 ml/min through serially-connected Discovery BIO GFC 500 (5 cm × 7.8 mm; Sigma) and Superose 6 (10/300GL; GE Biosciences) columns equilibrated with 150 mM NaCl, 10 mM Tris-HCl (pH 7.4), and 0.02% NaN_3 on a Gilson HPLC system essentially as described (5). Cholesterol levels were determined using an enzymatic colorimetric reaction by mixing the column effluent with a pump-delivered detection kit (Roche; 1:1 in column buffer at 0.2 ml/min) in a 0.6 ml knitted reactor coil (3 m × 0.5 mm) submerged in a 37°C water bath. Chromatograms were recorded at 505 nm and integrated using Geminyx 1.91 software (GOEBEL GmbH).

Supplemental References

1. Zhou Z, et al. Lipoprotein-derived lysophosphatidic acid promotes atherosclerosis by releasing CXCL1 from the endothelium. *Cell Metab*. 2011;13(5):592-600.
2. Grimson A, Farh KK-H, Johnston WK, Garrett-Engele P, Lim LP, Bartel DP. MicroRNA targeting specificity in mammals: determinants beyond seed pairing. *Mol Cell*. 2007;27(1):91-105.
3. Betel D, Wilson M, Gabow A, Marks DS, Sander C. The microRNA.org resource: targets and expression. *Nucleic Acids Res*. 2008;36(suppl 1):D149-D153.
4. Griffiths-Jones S, Saini HK, van Dongen S, Enright AJ. miRBase: tools for microRNA genomics. *Nucleic Acids Res*. 2008;36(Database issue):D154-158.
5. Parini P, Johansson L, Broijersen A, Angelin B, Rudling M. Lipoprotein profiles in plasma and interstitial fluid analyzed with an automated gel-filtration system. *Eur J Clin Invest*. 2006;36(2):98-104.